

Lasers in Manufacturing Conference 2019

# Laser polishing of Aluminum and Polyamide for dissimilar laser welded assemblies

Mahdi Amne Elahi<sup>a\*</sup>, Marcus Koch<sup>b</sup>, Peter Plapper<sup>a</sup>

<sup>a</sup>University of Luxembourg, 6, rue Coudenhove-Kalergi, L-1359 Luxembourg

<sup>b</sup>INM – Leibniz Institute for New Materials Campus D2 2, 66123 Saarbrücken Germany

---

## Abstract

In the present study, laser macro polishing on both Aluminum (Al) and Polyamide (PA) was investigated as a pre-treatment process for laser welding. To apply the laser polishing on Al and PA we used continuous wave (CW) fiber and CO<sub>2</sub> lasers, respectively. The samples were then welded in an overlap configuration. The results show that applying laser polishing in an atmospheric condition generates a nano-structured oxide layer generated on the Al surface. This layer represents much lower and isotropic roughness. In addition, considering the polishing of PA surface, some significant changes in the structure of the polished area are observed compared to as-received condition; however, there is no significant alteration in the surface chemistry. The alteration of surface structure can be attributed to a different crystallinity state. The modification of the Al surface is mainly responsible for improving tensile-shear load of the joint; however, modification of the PA surface can also contribute to the further improvement of the tensile-shear load and change the mechanism of failure.

Keywords: laser welding; laser macro polishing; nano-structured oxide layer; crystallinity.

---

## 1. Introduction

Developing hybrid components from lightweight materials like Al and PA is being well addressed over the past years specially in automotive and aerospace industries. Several processes have been developed to provide strong and reliable bonding between dissimilar materials. Among them, mechanical, adhesive and thermal joining are the main categories [Moldovan et al.]. Thanks to the unique advantages of laser welding like exceptional control over heat input or automation capability, joining metals to polymers with the laser

---

\* Corresponding author. Tel.: +350-466644-5885; fax: +352-466644-35885.

E-mail address: mahdi.amneelahi@uni.lu

beam have gained a considerable attention over the past few years. Heckert et al. reported that to achieve a load-bearing metal-polymer joint with the laser beam, the metal surface has to be pre-treated before the laser welding. To accomplish the mentioned pre-treatment on the metal side, several studies have been reported. Most of them are based on structuring the metal surface with different shapes and scales [Heckert et al., Schricker et al., Rodríguez-Vidal et al., Hopmann et al., and Zhang et al.]. Heckert et al. reported the effect of macroscopic, microscopic and nanoscopic surface structures of the Al on the shear strength.

There are few other studies, which are based on chemical preparation of the metal surface [Lamberti et al., Zhang et al.]. Lamberti et al. concluded that the effect of mechanical interlocking is not the principal cause for the bonding and reported the main effect of physicochemical interaction based on hydrogen bonds. Zhang et al. reported the chemical bonding of Al-O-PA6 after anodizing pre-treatment of the Al surface.

However, the lack of a systematic research to minimize the influence of mechanical interlocking and promote the chemical bonding between the metal and the polymer surfaces is present. Besides, the mechanical properties of the metal/polymer joints are not comparable to the base materials with the reported pre-treatments. It also worth mentioning that except for few studies [Arai et al.], most of the researchers tried surface pre-treatments only on the metal surface and the effect of polymer surface treatment is quite vague.

This study presents the effect of the laser polishing pre-treatment on both Al and PA surfaces before laser welding. The results show that a reliable joint is achieved based on chemical bonding at the interface of Al/PA and in optimum parametrical condition, the joint will be stronger than the base metal.

## 2. Experimental procedure

### 2.1. Laser Polishing (LP) process

In this study, PA 6.6 (75×25×4 mm) and 1050-H24 Al alloy (60×30×0.5 mm) were selected for welding in an overlap configuration. For the pre-treatment process, laser polishing (LP) were applied in atmospheric condition on the surface of the sample using continuous wave (CW) laser beam. Figure 1 illustrates the schematic description of the LP process with the corresponding parameters investigated to optimize the process for Al and PA separately.

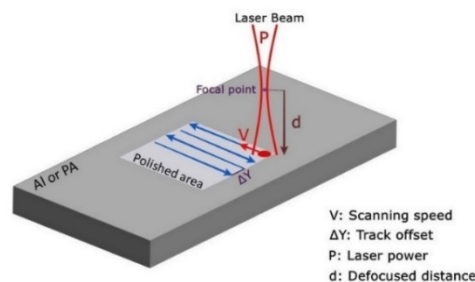


Fig. 1. LP process for Al or PA surface.

For the LP process of the Al samples, we used a fiber laser (TruFiber 400) with a near-infrared wavelength of 1070 nm. On the other hand, for PA polishing a CO<sub>2</sub> laser (laser station TM020+) with the wavelength of approximately 10.6 μm and max power of 25 W was used. The laser polishing parameters investigated for both materials are practically similar but not equal in value.

## 2.2. Laser welding

For the laser welding process, we used the same fiber laser. The fiber laser has been combined with a Scanlab HS20 2D f- $\theta$  scanner head so the beam quality of  $M^2=1.03$  and the spot size of  $30\text{ }\mu\text{m}$  were achieved. Figure 2 depicts the overview of sample positioning in the fixture, which is used to implement laser welding in atmospheric condition.

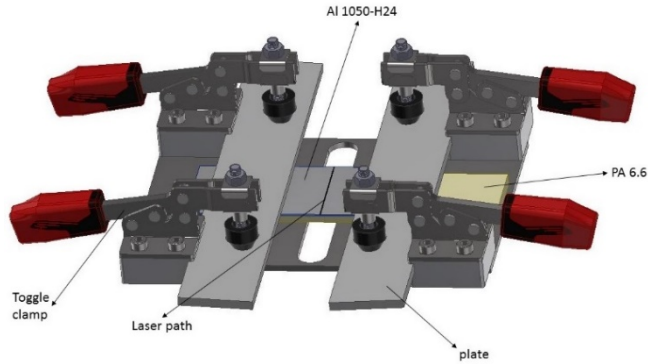


Fig. 2. The fixture implemented for laser welding.

As is clear from figure 2, the welding between Al and PA is achieved via conduction joining, therefore, to better control the input energy that is conducted to the PA surface, the spatial and temporal heat inputs were optimized for the welding process. Figure 3 shows the spatial and temporal modulations of the laser beam. It worth mentioning that all samples have been welded in an identical configuration.

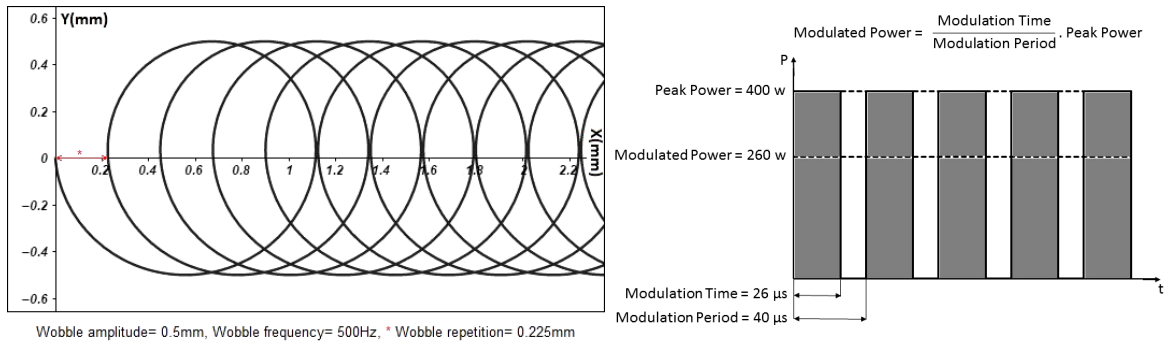


Fig. 3. Spatial (left) and temporal (right) modulations of the laser beam.

## 2.3. Surface characterization

To study the samples before and after pre-treatment, Scanning Electron Microscopy (with FEI ESEM Quanta 400 FEG) was used. The results consist of Secondary Electrons (SE) and Backscattered Electrons (BSE) images in addition to the chemical analysis of Energy-dispersive X-ray Spectroscopy (EDS) with EDAX Genesis V6.04. Optical Microscopy (OM) (with Leica DM 4000 M) was also used for some of the samples and to evaluate the mechanical properties of the joints the tensile-shear test using a Zwick/Roell machine with the

maximum force of 5KN was applied at the constant speed of 2.5 mm/min. The surface roughness of the samples was also studied by roughness measurement using a Mitutoyo SJ-500P based on ISO 4288-1996. The reported values are representative of at least five individual measurements.

The cross-sections of samples were prepared by using a conventional metallography process including mounting, progressive grinding with abrasive paper, and polishing with diamond suspension or alumina. In order to avoid the presence of ordinary contaminations, the surfaces of all samples have been cleaned with ethanol before doing further treatments. Then, to define the dryness state of the PA, the samples have been dried enough at 35°C in a vacuum oven before further processing.

### 3. Results and discussions

#### 3.1. Characterization of Al samples before and after laser polishing

Figures 4-a and 4-b illustrate the structure of the Al surface and the corresponding EDS analysis in as-received condition respectively and Figures 5a and 5b depict the similar characterizations for laser polished condition.

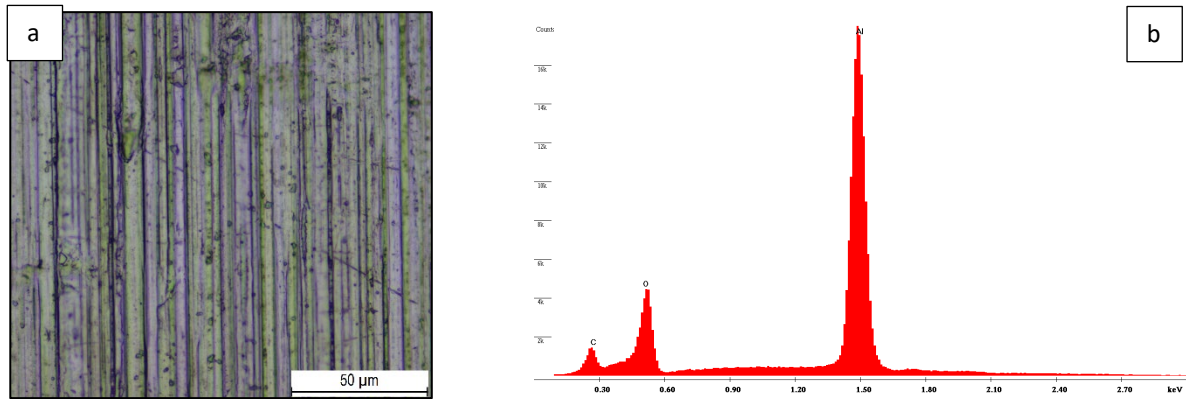


Fig. 4. a) OM image of Al surface in as-received condition and b) corresponding EDS analysis.

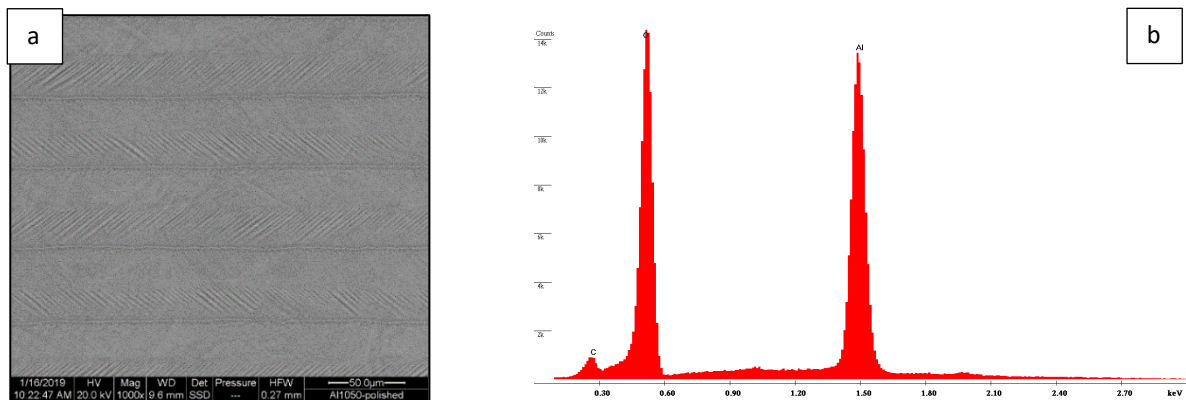


Fig. 5. a) BSE image of Al surface in laser polished condition and b) corresponding EDS analysis.

By analyzing the surface of the Al samples before and after the LP process, the alteration in surface roughness and chemistry is quite clear. The high roughness of the as-received sample in the rolling direction (figure 4-a) disappears after the LP process (figure 5-a). A brief comparison between EDS analysis of the samples before and after the LP process (figures 4-b and 5-b), shows a substantial increase of oxygen content after the LP process. As the current LP process includes surface melting under atmospheric condition, the mentioned high oxygen content is attributed to the presence of aluminum oxide. A slight cleaning effect is also visible by the LP process. As-received condition has more carbon content compared to the polished samples. Figure 6 represents the structure of the Al oxide layer and its thickness. The present nano-structured oxide layer has a thickness of approximately 2  $\mu\text{m}$ .

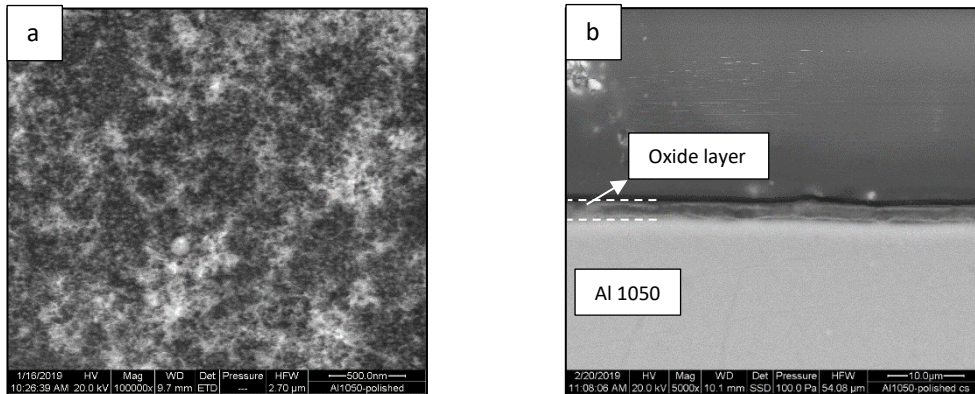


Fig. 6. a) SE image of Al surface after the LP process and b) SE image of the cross-section of the laser polished the Al sample.

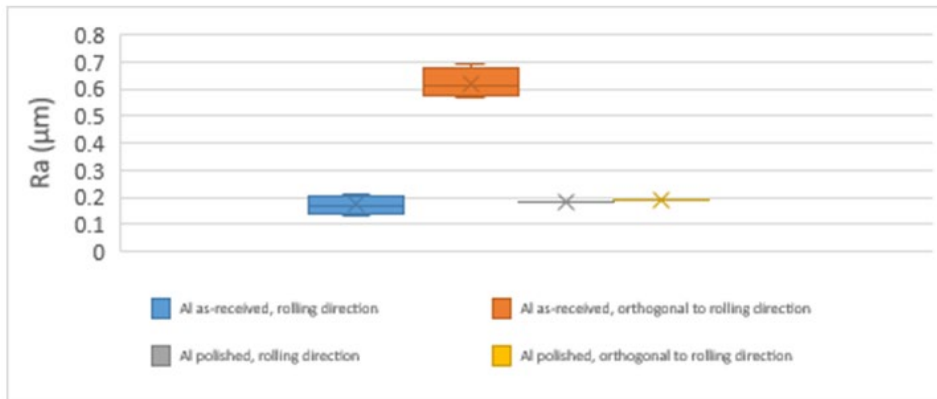


Fig. 7. Roughness measurement of the Al surface.

Figure 7 depicts the results of roughness measurements for the Al surfaces before and after the LP process. As was also noticed in Figures 4 and 5, a relatively high roughness in the direction orthogonal to the rolling direction is quite visible; however, after the LP process the roughness drops significantly in the direction orthogonal to rolling direction. Thereby it is comparable to the roughness of the rolling direction or in other words, the roughness is quite isotropic after the LP process.

### 3.2. Characterization of PA samples before and after laser polishing

Figure 8 shows the PA surface characterizations before the pre-treatment. As this figure shows, the PA surface is smooth and there are no visible impurities in the EDS analysis of the PA.

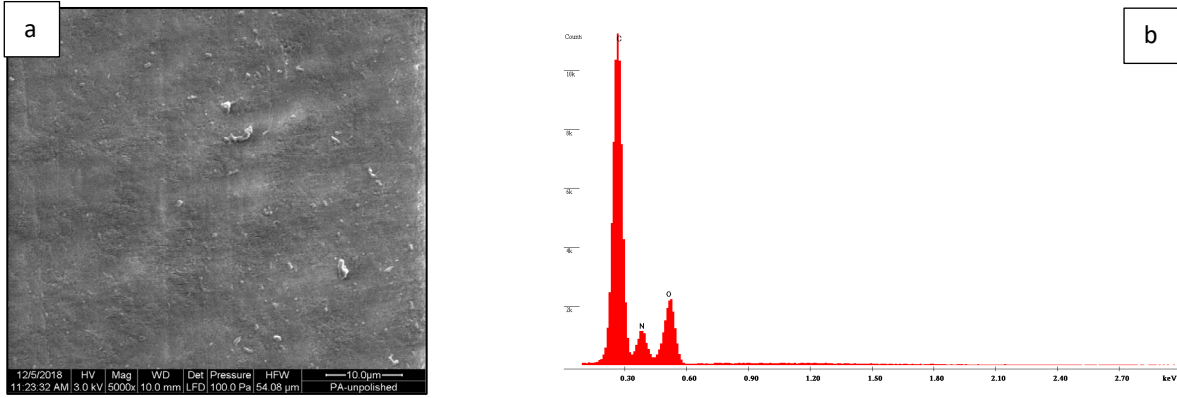


Fig. 8. a) SE image of the PA surface in as-received condition and b) corresponding EDS analysis.

Figure 9 illustrates the observation of spherulites on the PA surface after the LP process (a) and the cross-section of the treated sample (b). As can be seen, by implementing the LP process on PA, the surface structure has been altered and the thickness of this alteration is approximately 30 μm. There is no significant difference between the EDS analysis of samples before and after the LP process, indicating that the main effect of the LP process on the PA surface with current configuration is mainly related to the structure or in other words, the crystallinity state of the PA surface. Further investigations on this structural alteration will be studied.

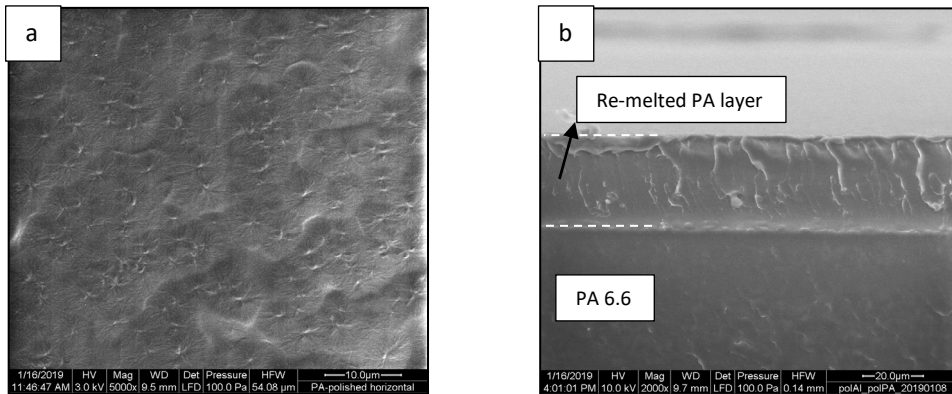


Fig. 9. a) Presence of spherulites on the PA sample surface after the LP process and b) the cross-section of the polished sample.

Figure 10 also shows the roughness measurements of the PA samples and unlike to the effect of the LP process on the Al surface, a slight increase in roughness occurs on the PA surface after the LP process; however, the isotropy in surface roughness is still present. The increase in surface roughness is probably due to spherulites formation.



Fig. 10. Roughness measurement of the PA surface.

Considering the results of roughness measurement (Figures 7 and 10), we can conclude that the main contributor to the joint strength will be chemical bonding and the effect of mechanical interlocking will not be significant.

### 3.3. Characterization of the welded samples

#### 3.3.1. Tensile-shear test

To categorize the condition of the samples effectively regarding different pre-treatment conditions, Table 1 shows the coding of the welded samples with different surface pre-treatments.

Table 1. Sample coding with Al and PA surface pre-treatments.

Sample categories	Al surface	PA surface
<b>A</b>	As-received	As-received
<b>B</b>	Laser polished	As-received
<b>C</b>	As-received	Laser polished
<b>D</b>	Laser polished	Laser polished



Figure 11 demonstrates the tensile shear load of the laser-welded specimens. The effect of the surface pre-treatment by the LP process on the tensile-shear load is observable. Having in mind that laser polishing of the Al surface not only reduces the surface roughness thereby making it clearly isotropic but also creates an artificial oxide layer. On the contrary, laser polishing of the PA will slightly increase the surface roughness and clearly alters the surface structure; nevertheless, the alteration of surface chemistry is not obvious. Considering tensile-shear test results, the main contributors to improve the mechanical properties of the joint is polishing of the Al surface with the laser beam and the PA laser polishing can be only effective when the latter is combined with Al laser polishing.

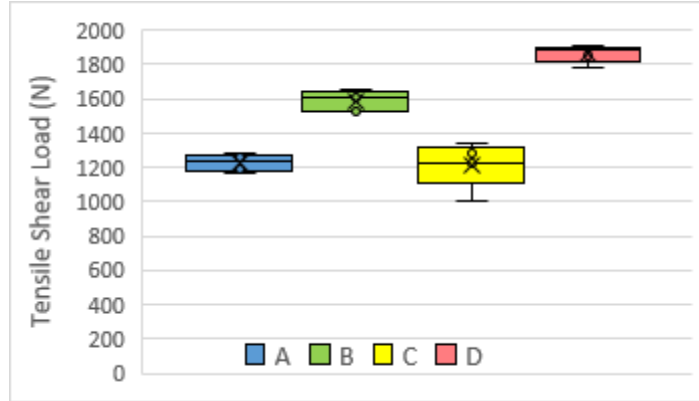


Fig. 11. Tensile-shear load of the samples with different combinations of surface treatments.

### 3.3.2. Fracture surfaces

Figure 12 shows the SE images of the Al samples (as-received and laser polished condition) in a tilted configuration after the tensile shear test to investigate a brief overview of the whole 25 mm of contact between the Al and the PA after the mechanical test. In figure 12-a, a mixture of adhesive and cohesive failures in the PA surface happened. In other words, the molten PA cannot effectively wet the as-received Al surface and the effective cross-section between the Al and the PA after welding is only limited to distributed droplets. These droplets would be formed in the spots where the Al surface is thermally or chemically favorable to bond with molten PA. This can also explain the reason for a slight reduction of the tensile-shear load regarding the category C compared to the category A in Figure 11.



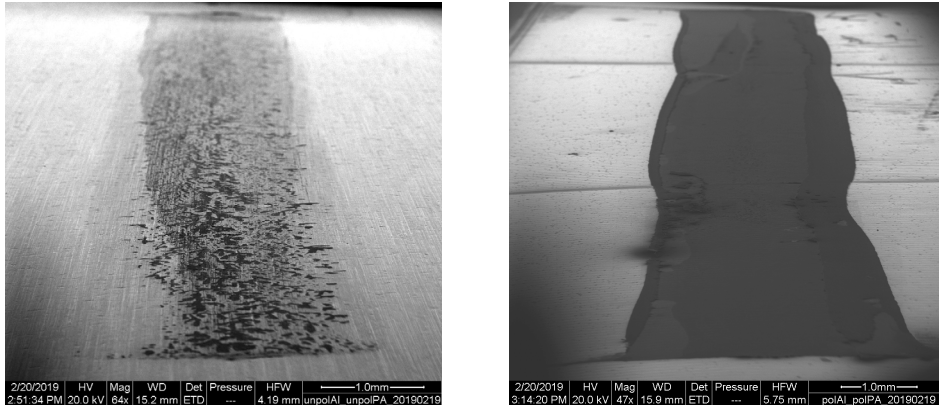


Fig. 12. The Al surface after tensile shear test of welded specimen a) Category A of surface pre-treatment, b) Category D of surface pre-treatment.

Considering the categories A and C, the Al surface does not have the artificial oxide layer therefore the molten PA will not wet the Al surface effectively. On the other hand, the roughness of the Al surface in as-received condition does not provide a uniform heat transfer from the Al to the PA. Having in mind the slight increase of the PA surface roughness in the category C compared to the category A, the smallest contact area and the most non-uniform heat distribution from the Al to the PA is present in the category C. Therefore, changing the structure of PA on the surface cannot be decisive and relatively the lowest mechanical properties of the welded specimens can be expected for the category C. It should be also noted that the individual droplets of the PA on discontinuous cross section (the categories A and C) act as stress concentration areas and significantly deteriorate the mechanical properties of the joint.

Referring to the category B, the Al surface possesses the artificial oxide layer; therefore, a perfect wettability of the molten PA and Al surface is expected. Figure 12-b also shows a significant improvement of the wettability between the Al surface and molten PA because of the LP process.

Now considering the samples of the category D, they have the advantage of the Al surface treatment, which can compensate the slight increase of the PA surface roughness and therefore the alteration of the PA surface structure can be effective and further increase the tensile-shear load of the joint. In other words, having a different crystallinity state on the PA surface has improved the tensile-shear strength.

Figure 13 depicts the cross-section of welded Al/PA in the category D. Due to very low roughness of the Al and PA surfaces the heat conduction from the Al to the PA is uniform therefore, at the cross-section the presence of bubbles formation because of PA degradation is not visible. Lack of bubbles at the interface of Al/PA is another contributor to the improvement of the tensile-shear load.

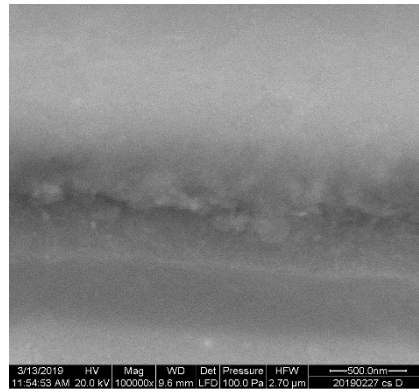


Fig. 13. The cross-section of welded Al/PA in the category D.

Finally, by optimization of the welding parameters, the joint is stronger than the base metal and the value of tensile strength is comparable to the Al 1050. Figure 14 shows the appearance of the welded specimen in optimum condition after the tensile-shear test.

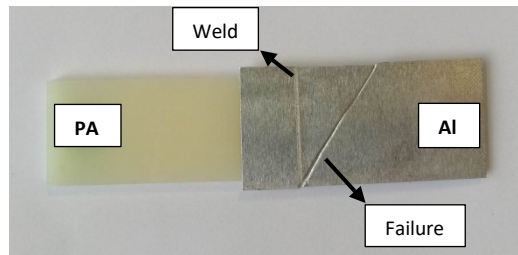


Fig. 14. Failure of the base metal during the tensile-shear test in the optimum condition of welding of D category.

#### 4. Conclusions

We present the following conclusions based on the results presented in this paper of LP process of the Al and the PA surfaces for dissimilar laser welded assemblies:

1. Laser polishing process of the Al surface will significantly reduce the roughness in the direction orthogonal to the rolling direction and makes the surface roughness isotropic while the laser polishing of PA will slightly increase the surface roughness with improving the roughness isotropy. Therefore the main contributors to the mechanical properties of the joint between Al and PA, is chemical bonding.
2. By implementing the laser polishing in atmospheric condition, an artificial oxide layer is developed on the Al surface; however, for the laser polishing of the PA no significant alteration in surface chemistry is visible with EDS, nevertheless the alteration of the surface structure is clearly observed. This observation can be referred to a different crystallinity state.
3. Generating an artificial oxide layer on Al is an effective way to improve wettability between the molten PA and the Al regardless of the surface roughness. The low surface roughness after the LP process provides uniform heat conduction from the Al to the PA. The uniform heat distribution at the given welding parameters prevents PA degradation and therefore bubbles formation at the interface.
4. The joint of laser-welded assembly of Al and PA is stronger than the base metal if the laser polishing is implemented on Al and the PA surfaces in optimum condition.

## Acknowledgement

The presented work is based on “Process Innovation for Sensors in Mobile Applications Based on Laser Assisted Metal-Plastic Joining” project (AFR-PPP grant, Reference 11633333). The authors would like to thank the support of Luxembourg National Research Fund (FNR) and acknowledge Cebi International S.A. as the industrial partner of the project.

## References

- Moldovan, E., Tiorean, M. H., Stanciu, E. M., 2017. Overview of Joining Dissimilar Materials, *Metals and Polymers* 10, p. 39-46.
- Heckert A., Singer C., Zaeh M. F., 2015. Pulsed Laser Surface Pre-Treatment of Aluminium to Join Aluminium - Thermoplastic Hybrid Parts, *Lasers in Manufacturing Conference*.
- Heckert A., Zaeh M. F., 2014. Laser surface pre-treatment of aluminium for hybrid joints with glass fibre reinforced thermoplastics. *Physics Procedia* 56(C), p. 1171–81.
- Schricker, K., Stambke, M., Bergmann, J. P., Bräutigam K., Henckell P., 2014. Macroscopic surface structures for polymer-metal hybrid joints manufactured by laser based thermal joining. *Physics Procedia* 56(C) p. 782–790.
- Rodríguez-Vidal E., Sanz C., Soriano C., Leunda J., Verhaeghe G., 2016. Effect of metal micro-structuring on the mechanical behavior of polymer-metal laser T-joints, *Journal of Materials Processing Technology* 229, p. 668-677.
- Hopmann C., Kreimeier S., Keseberg J., Wenzlau C., 2016. Joining of Metal-Plastics-Hybrid Structures Using Laser Radiation by Considering the Surface Structure of the Metal, *Hindawi Publishing Corporation Journal of polymers*, p. 1-10.
- Zhang Z., Shan J., Tan X., Zhang J., 2017. Improvement of the laser joining of CFRP and aluminum via laser pre-treatment. *International Journal Advanced Manufacturing Technology* 90, p. 3465-3472.
- Lamberti, C., Solchenbach, T., Plapper, P., Possart, W., 2014. Laser assisted joining of hybrid polyamide-aluminum structures. *Physics Procedia* 56(C):p. 845-853.
- Zhang Z., Shan J., Tan X., Zhang J., 2016, Effect of anodizing pretreatment on laser joining CFRP to aluminum alloy A6061, *International Journal of Adhesion & Adhesives* 70, p. 142-151.
- Arai, S., Kawahito, Y., Katayama, S., 2014. Effect of surface modification on laser direct joining of cyclic olefin polymer and stainless steel, *Materials and design* 59, p. 448-453.